Lyapunov-Based Economic Model Predictive Control for Online Model

Discrimination

Henrique Oyama^a, Helen Durand^{*,a}

^aDepartment of Chemical Engineering and Materials Science, Wayne State University, Detroit, MI 48202, USA.

Abstract

Economic model predictive control (EMPC) is a flexible control design strategy that can be modified to

achieve many operating goals while also ensuring safe operation (e.g., by adding Lyapunov-based stability

constraints to form Lyapunov-based EMPC, or LEMPC). Prior works have investigated LEMPC capabil-

ities for achieving goals online beyond optimizing process economics, including aiding in model structure

selection to benefit model-based control system design since the accuracy and quality of the process model

are important for achieving an expected performance from such systems. This work further probes the

capabilities of LEMPC to accomplish multiple objectives during process operation, including aiding in the

discrimination between mechanistic models online. In particular, several rival mechanistic models may

explain the existing data. To discard models from this set that do not fully represent the actual process, a

new set of "online experiments" can be conducted to collect more information. However, additional experi-

mentation may be costly and unsafe to be performed. LEMPC can aid in performing online data collection

when discrimination between mechanistic models is needed, with the flexibility to ensure safety as the data

is gathered and trade off the data-gathering goal for cost considerations. Motivated by this, we discuss how

LEMPC can be designed to automatically and dynamically collect data that is useful for the selection of

mechanistic models from among a set of possibilities. A chemical process example is used to clarify benefits

and limitations of LEMPC for promoting online model discrimination.

Key words: Economic model predictive control, nonlinear systems, model discrimination

*Corresponding author: H. Durand, Tel: +1 (313) 577-3475; E-mail: helen.durand@wayne.edu.

1. Introduction

Economic model predictive control (EMPC)¹ is an optimization-based control strategy that has found numerous applications, including in bioreactor systems,² periodic process operation,³ and building temperature control. One of its key characteristics is flexibility due to the fact that it is formulated as a general nonlinear or nonconvex optimization problem, and that its purpose is to facilitate operating objectives beyond tracking a steady-state or reference. EMPC's name focuses on its ability to optimize economic performance online; however, it is also capable of achieving a variety of other online objectives, such as attempting to gather data that might be indicative of process model structure⁵ (which can aid in developing and selecting mechanistic models which may or may not have data-driven components, i.e., parameter values obtained based on a process dataset). Another way of conceptualizing the use of real-time control for aiding in selecting an appropriate model structure is to assume that already, a number of mechanistic model candidates have been proposed, and that it is desired to determine which of them provides a sufficient fit to additional process data. In this work, we demonstrate that LEMPC can also be formulated to carry out this goal, further demonstrating its flexibility for performing a variety of tasks safely and online, and thereby suggesting that EMPC may be an interesting technology to consider for next-generation manufacturing goals such as full plant autonomy⁶ where the capability of a controller to be able to carry out a large number of online tasks can be attractive.

The potential benefit for full plant autonomy of a controller which can aid in model-building tasks in a variety of ways is that system modeling by engineers can be a time-consuming and at times challenging task. Modeling strategies (e.g., system identification) often rely on data collected *a priori* to indicate an appropriate model form/structure for representing the behavior of a specific dynamical system, or in cases where deciding upon an appropriate mechanistic model form is too time-consuming or expensive, different engineering strategies have been proposed such as assuming a gray-box or hybrid model structure that integrates physics-based components with empirical model parts.^{7,8,9} However, after an investigation and model identification procedure is applied, based on the available experimental data and potentially physical insights, a set of plausible mechanistic models may be capable of explaining the available information.¹⁰ This situation requires new online experiments to select a model from among a set of seemingly good

mechanistic models via additional data. An EMPC formulation that automatically chooses which data to collect as part of online "experimentation" for discriminating between rival mechanistic models while ensuring safe operation may be beneficial, which extends the "EMPC toolbox" to include the capability of EMPC to aid in online model discrimination.

Studies addressing experiment design for engineering systems have been conducted which focused on parameter estimation techniques (e.g., 11) or discrimination between competing models (e.g., 12,13). For example, in, 11 an iterative parameter identification methodology based on a class of polynomial models has been utilized to apply optimal control sequences to the system for identification experiment design while the model complexity is progressively increased. In, 12 an online model-based design of experiment approach was proposed for model selection to identify the best model from a list of candidates in an autonomous reactor platform. Data-supported computational modeling of engineering systems often involves model identification (e.g., parameter estimation or model fitting), model discrimination, and model validation. 14,15 However, as engineers move toward greater autonomy of control systems, it would be beneficial to design automated optimal input sequences for collecting data online which is most favorable for discriminating between different potential models while ensuring safe and high-performance operation inside the process operating region.

An important direction for safe and automated model discrimination is model-based control-assisted frameworks. An approach described as model predictive control (MPC) with dual features (i.e., the manipulated inputs are used both to control and explore the system) has been proposed (e.g., ^{16,17}). In, ¹⁶ a dual control scheme has been used to perform experimentation (sufficient excitation to the process) only when there is high uncertainty in the parameters or not enough information is available for parameter identification. In, ¹⁷ an adaptive dual model predictive controller has been proposed based on output error models parameterized using generalized orthogonal basis filters and applied to inject input excitation. In addition, a control design named model predictive control and identification has been developed in ¹⁸ and incorporates constraints that enforce persistent excitation. A stochastic MPC scheme proposed in ¹⁹ uses active model structure discrimination during process operation for closed-loop fault diagnosis. In the direction of exciting a system for exploration/exploitation, learning-based MPC or safe learning in control has also been investigated. ^{20,21,22} In, ²⁰ for example, a sequential exploration-exploitation approach has

been proposed that uses active learning in control to gather data and reduce dynamics uncertainty during an exploration step and then exploit the acquired information to perform the desired task while ensuring high-probability guarantees of satisfying safety constraints. In,²¹ a control architecture has been proposed that utilizes a model-free reinforcement learning algorithm to learn a controller with the control barrier function-based controller guiding policy exploration and ensuring safety during the learning process.

In the context of online model discrimination using model-based control-assisted designs, an EMPC framework, which can outperform conventional MPC schemes in terms of improving process profitability, may also be used for selecting mechanistic models online. In, an EMPC has been utilized to guide the process state to conditions over time which might suggest the form of a dynamic model (by, for example, attempting to hold one process variable constant while manipulating others). However, a challenge with the approach in is that the guidance to select helpful data for the model structure selection procedure is based on penalizing deviations of the predicted state from desired data in the objective function or enforcing a stabilization constraint to attempt to develop data which lies along the pathway from a given point toward the origin. This requires some a priori assessment of what the desired data might be. In the interest of making the discrimination between physics-based models automated and less costly, automatic techniques are needed for determining what the desired data should be.

This work seeks to suggest an automated technique for online control-assisted discrimination between mechanistic models (by discerning which mechanistic model structure may be most in accordance with the new online "experimental" data) to extend EMPC's capabilities. Because EMPC is not restricted to steady-state operation, it may also enable a flexible strategy for explicitly trading off economic performance and mechanistic model selection. A flexible type of EMPC with closed-loop stability constraints named Lyapunov-based economic model predictive control (LEMPC)²³ is used to formulate a technique for dynamically collecting desired data while accounting for process dynamics, safety, and process profitability. Specifically, since LEMPC is designed to operate the process within a pre-defined stability region, a model that allows good state predictions inside the stability region may be sufficient to guarantee the desired control performance and safe operation. In this case, mechanistic models may be able to be used by the LEMPC to predict the process state trajectory with acceptable accuracy inside the designed region of operation. We assume that mechanistic model candidates have already been suggested, but that the set of

mechanistic model possibilities remains to be discriminated between while ensuring closed-loop stability in a safe region of state-space. A chemical process example that illustrates aspects of the methodology is discussed.

2. Preliminaries

2.1. Notation

R corresponds to the set of real numbers. The Euclidean norm of a vector is indicated by $|\cdot|$ and the transpose of a vector x is denoted by x^T . A continuous function $\alpha:[0,a)\to[0,\infty)$ is said to be of class $\mathcal K$ if it is strictly increasing and $\alpha(0)=0$. Set subtraction is designated by $x\in A/B:=\{x\in R^n:x\in A,x\notin B\}$. Finally, a level set of a positive definite function V is denoted by $\Omega_\rho:=\{x\in R^n:V(x)\leq\rho\}$.

2.2. Class of Systems

The class of nonlinear systems considered is the following:

$$\dot{x}(t) = f(x(t), u(t), w(t)) \tag{1}$$

where $x \in X \subset R^n$ and $u \in U \subset R^m$ are the state and input vectors, respectively, in deviation variable form from the steady-state (x_s) and steady-state input of the system (u_s) ; $w \in W \subset R^z$ $(W := \{w \in R^z \mid |w| \le \Theta, \ \Theta > 0\})$ is the disturbance vector and f is locally Lipschitz on $X \times U \times W$. We consider that the "nominal" system of Eq. 1 $(w \equiv 0)$ has its origin at the equilibrium point (i.e., f(0,0,0) = 0) and is stabilizable such that there exists an asymptotically stabilizing feedback control law $h_p(x)$, a sufficiently smooth Lyapunov function V(x), and class K functions $\alpha_i(\cdot)$, i = 1, 2, 3, 4, where:

$$\alpha_1(|x|) \le V(x) \le \alpha_2(|x|) \tag{2a}$$

$$\frac{\partial V(x)}{\partial x} f(x, h_p(x), 0) \le -\alpha_3(|x|) \tag{2b}$$

$$\left| \frac{\partial V(x)}{\partial x} \right| \le \alpha_4(|x|) \tag{2c}$$

$$h_p(x) \in U \tag{2d}$$

 $\forall x \in D \subset \mathbb{R}^n$ (D is an open neighborhood of the origin). We define $\Omega_{\tilde{\rho}} \subset D$ to be the stability region of the nominal closed-loop system under the controller $h_p(x)$ and require that it be chosen such that $x \in X$, $\forall x \in \Omega_{\tilde{\rho}}$. We consider that state measurements are available continuously, but are only used by a controller at discrete sampling times for computing a control action.

In this work, we consider the following nonlinear model candidates represented by nonlinear ordinary differential equations:

$$\dot{x}_{q,i}(t) = f_{NL,i}(x_{q,i}(t), u_{q,i}(t)) \tag{3}$$

where $f_{NL,i}$ is a locally Lipschitz nonlinear vector function in $x_{q,i} = [x_{q,i1} \ x_{q,i2} \ \dots \ x_{q,in}]^T \in X \subset R^n$ and in the input $u_{q,i} = [u_{q,i1} \ u_{q,i2} \ \dots \ u_{q,im}]^T \in U_{q,i} \subset \mathbb{R}^m$ (both in deviation variable form from the steady-state (which shares the same x_s of Eq. 1) and steady-state input $u_{q,i,s}$ of the system of Eq. 3) with $f_{NL,i}(0,0) = 0$ for all i. The index $i = 1, 2, \ldots$, is used to reflect that different nonlinear models may be used over time. We consider nonlinear models for which the origin can be rendered asymptotically stable by a stabilizing feedback control law $(h_{NL,i}(x_{q,i}) = [h_{NL,i,1}(x_{q,i}) \ h_{NL,i,2}(x_{q,i}) \ \dots \ h_{NL,i,m}(x_{q,i})]^T)$, considering a sufficiently smooth Lyapunov function and class \mathcal{K} functions $\hat{\alpha}_i(\cdot)$, i = 1, 2, 3, 4, where:

$$\hat{\alpha}_1(|x_{q,i}|) \le \hat{V}_i(x_{q,i}) \le \hat{\alpha}_2(|x_{q,i}|) \tag{4a}$$

$$\frac{\partial \hat{V}_i(x_{q,i})}{\partial x_{q,i}} f_{NL,i}(x_{q,i}, h_{NL,i}(x_{q,i})) \le -\hat{\alpha}_3(|x_{q,i}|)$$

$$\tag{4b}$$

$$\left| \frac{\partial \hat{V}_i(x_{q,i})}{\partial x_{q,i}} \right| \le \hat{\alpha}_4(|x_{q,i}|) \tag{4c}$$

$$h_{NL,i}(x_{q,i}) \in U_{q,i} \tag{4d}$$

 $\forall x_{q,i} \in D_{q,i}$ (an open neighborhood of the origin). We define $\Omega_{\rho_i} \subset D_{q,i}$ (chosen such that $x_{q,i} \in X$, $\forall x_{q,i} \in \Omega_{\rho_i} \subset \Omega_{\tilde{\rho}}$) to be the stability region. There are positive constants \hat{L}'_{x_i} , and \hat{M}_{f_i} , $\forall x_1, x_2, x_{q,i} \in \Omega_{\tilde{\rho}}$ and $u_{q,i} \in U_{q,i}$, such that:

$$\left| \frac{\partial \hat{V}_i(x_1)}{\partial x_1} f_{NL,i}(x_1, u_{q,i}) - \frac{\partial \hat{V}_i(x_2)}{\partial x_2} f_{NL,i}(x_2, u_{q,i}) \right| \le \hat{L}'_{x_i} |x_1 - x_2|$$
 (5a)

$$|f_{NL,i}(x_{q,i}, u_{q,i})| \le \hat{M}_{f_i} \tag{6}$$

Finally, because f is a locally Lipschitz function of its arguments, we can write the following for all $x_1, x_2 \in \Omega_{\tilde{\rho}}, u \in U, w \in W$, and L_x, L'_x, L_w, L'_w , and M_f as positive constants:

$$|f(x_1, u, w) - f(x_2, u, 0)| \le L_x |x_1 - x_2| + L_w |w|$$
(7a)

$$\left| \frac{\partial V(x_1)}{\partial x} f(x_1, u, w) - \frac{\partial V(x_2)}{\partial x} f(x_2, u, 0) \right| \le L_x' |x_1 - x_2| + L_w' |w| \tag{7b}$$

$$|f(x, u, w)| \le M_f \tag{8}$$

2.3. Economic Model Predictive Control

 $\mathrm{EMPC^{24}}$ is an optimization-based control design for which the control actions are computed via the following optimization problem:

$$\min_{u(t)\in S(\Delta)} \int_{t_k}^{t_{k+N}} L_e(\tilde{x}(\tau), u(\tau)) d\tau$$
(9a)

s.t.
$$\dot{\tilde{x}}(t) = f(\tilde{x}(t), u(t), 0)$$
 (9b)

$$\tilde{x}(t_k) = x(t_k) \tag{9c}$$

$$\tilde{x}(t) \in X, \, \forall \, t \in [t_k, t_{k+N})$$
 (9d)

$$u(t) \in U, \ \forall t \in [t_k, t_{k+N}) \tag{9e}$$

where N is called the prediction horizon, and u(t) is a piecewise-constant input trajectory with N pieces, where each piece is held constant for a sampling period with time length Δ . The economics-based stage cost L_e of Eq. 9a is evaluated throughout the prediction horizon using the future predictions of the process state \tilde{x} from the model of Eq. 9b (the nominal model of Eq. 1) initialized from the state measurement at t_k (Eq. 9c). The process constraints of Eqs. 9d-9e are state and input constraints, respectively. The optimization problem is solved every Δ time units (at each sampling time t_k) such that the first of the N pieces of the optimal input vector trajectory is applied to the process. A type of EMPC called Lyapunov-based EMPC (LEMPC²³) incorporates the following additional constraints:

$$V(\tilde{x}(t)) \le \tilde{\rho}_e, \ \forall t \in [t_k, t_{k+N}), \ \text{if } x(t_k) \in \Omega_{\tilde{\rho}_e}$$
 (10a)

$$\frac{\partial V(\tilde{x}(t_k))}{\partial x} f(\tilde{x}(t_k), u(t_k), 0) \le \frac{\partial V(\tilde{x}(t_k))}{\partial x} f(\tilde{x}(t_k), h_p(x(t_k)), 0), \quad \text{if } x(t_k) \in \Omega_{\tilde{\rho}}/\Omega_{\tilde{\rho}_e}$$
(10b)

where $\Omega_{\tilde{\rho}_e} \subset \Omega_{\tilde{\rho}}$ makes $\Omega_{\tilde{\rho}}$ forward invariant under the controller of Eqs. 9-10.

3. Online Control-Assisted Mechanistic Model Structure Discrimination Using LEMPC

Prior work⁵ in our group described how data that might reveal aspects of what a reasonable model structure for a system's dynamics is could be attempted to be obtained using a formulation of LEMPC that penalizes deviations from the desired data in the objective function and enforces the constraint of Eq. 10b at intermittent times. However,⁵ did not provide an automated mechanism for determining what data to gather (i.e., what the "desired" data should be). In this work, we consider that one of the goals of designing

optimal control sequences for selecting an appropriate mechanistic model is to discriminate among possible mechanistic models for a system that are consistent with its behavior. The "desired data," then, is that which reveals which of a set of potential mechanistic model structures is consistent with the process behavior. The flexibility of LEMPC allows it to attempt to gather this data in a manner that guarantees closed-loop stability throughout the data-gathering process. Particularly, we propose an LEMPC-assisted mechanistic model discrimination procedure that incorporates closed-loop stability guarantees via the constraints of Eqs. 10a-10b with the ability to gather meaningful data without compromising closed-loop stability. The fact that the objective function of LEMPC does not impact stability or feasibility guarantees allows it to be modified if desired to attempt to gather different data than might occur under normal operation for model discrimination. In the following subsections, we formalize this control concept.

3.1. LEMPC for Discriminating Between Mechanistic Models: Formulation

To achieve the data-gathering goals described above and attempt to quickly discern between potential models, the control design takes the form of the LEMPC in Eqs. 9-10 but enforces certain criteria (which will be clarified in Section 4.3) on each of a set of $|M_c|$ mechanistic models, where $|M_c|$ represents the cardinality of a set M_c of model candidates. The objective function of the LEMPC can be modified if it is considered that an economics-based objective function does not cause the computed control actions to cause the state predictions between different models to be sufficiently different (when it is not known which model may provide the most accurate state predictions, an economics-based objective function might minimize the sum of all of the costs which might be obtained under the different models, where we denote this sum by $\sum_{i=1}^{|M_c|} L_e(\tilde{x}_{q,i}(\tau), u_{q,1}(\tau)))$. For example, to modify the objective function, a term could be added to the stage cost that penalizes "closeness" of the trajectories of the states of two of the process models from one another (to attempt to cause the LEMPC to maximize the difference between the state predictions from the different models under the inputs that it computes). The resulting two terms in the objective function may be weighted by binary parameters (denoted by β_1 and β_2 in the following) to enable activation of either a profit-maximizing mode or a data-gathering-focused mode independently. This provides some capability to collect non-routine operating data when minimizing costs does not provide data that enables models to be

discriminated. The formulation of the LEMPC just described is as follows:

$$\min_{u_{q,1}(\cdot)\in S(\Delta)} \int_{t_k}^{t_{k+N}} \left[\beta_1 \sum_{i=1}^{|M_c|} L_e(\tilde{x}_{q,i}(\tau), u_{q,1}(\tau)) - \beta_2 \sum_{i=1}^{|M_c|} \sum_{j=i+1}^{|M_c|} \gamma_{ij} |\tilde{x}_{q,i}(\tau) - \tilde{x}_{q,j}(\tau)|^2\right] d\tau \qquad (11a)$$

s.t.
$$\dot{\tilde{x}}_{q,i}(t) = f_{NL,i}(\tilde{x}_{q,i}(t), u_{q,i}(t)), i = 1, \dots, |M_c|, u_{q,i} = u_{q,1} + u_{q,1,s} - u_{q,i,s}$$
 (11b)

$$\tilde{x}_{q,i}(t_k) = x(t_k), i = 1, \dots, M_c \tag{11c}$$

$$\tilde{x}_{q,1}(t) \in X, \ \forall \ t \in [t_k, t_{k+N}) \tag{11d}$$

$$u_{a,1}(t) \in U_{a,1}, \ \forall t \in [t_k, t_{k+N})$$
 (11e)

$$\hat{V}_1(\tilde{x}_{q,1}(t)) \le \rho_{e,1}, \ \forall \ t \in [t_k, t_{k+N}) \ \text{if} \ \ \hat{V}_1(\tilde{x}_{q,1}(t_k)) \le \rho_{e,1}$$
 (11f)

$$\frac{\partial \hat{V}_{1}(\tilde{x}_{q,1}(t_{k}))}{\partial \tilde{x}_{q,1}} f_{NL,1}(\tilde{x}_{q,1}(t_{k}), u_{q,1}(t_{k})) \ \leq \frac{\partial \hat{V}_{1}(\tilde{x}_{q,1}(t_{k}))}{\partial \tilde{x}_{q,1}} f_{NL,1}(\tilde{x}_{q,1}(t_{k}), h_{NL,1}(\tilde{x}_{q,1}(t_{k})))$$

if
$$V_1(\tilde{x}_{q,1}(t_k)) > \rho_{e,1}$$
 (11g)

where L_e is the EMPC economics-based stage cost function (reflecting costs that must be minimized), $\tilde{x}_{q,i}$ and $\tilde{x}_{q,j}$ are the state predictions in deviation variable form from x_s based on the i-th and j-th model candidate, respectively, and $x(t_k)$ is the state measurement at t_k . $\beta_2 = 1$ corresponds to the activation of the data-gathering mode. However, both terms β_1 and β_2 may be set to 1 to attempt to account also for profitability measures while collecting closed-loop informative data. In this case, a trade-off between process economics and model discrimination is considered (e.g., if the system is already operating in an economically optimal fashion at steady-state and the maximization of the predicted state trajectories among all rival models happens away from this operating condition). In addition, each term corresponding to the magnitude difference between $\tilde{x}_{q,i}$ and $\tilde{x}_{q,j}$ in the double summation in the objective function of Eq. 11a can be weighted with γ_{ij} (which may aid with placing importance on certain terms or putting all terms on the same order of magnitude). $\rho_{e,1}$ is analogous to $\tilde{\rho}_e$ in Eq. 10, for the 1-th empirical model.

In this work, we assume that the stability regions for each of the models are nested such that the i=1 model has the smallest stability region, followed by that for i=2 (which fully contains that for i=1), and so forth. The stability region for the $i=|M_c|$ model is the largest and contains every one of the other stability regions for $i<|M_c|$, and $\Omega_{\rho_{low}}\subseteq\Omega_{\rho_i}$ (where $\Omega_{\rho_{low}}=\Omega_{\rho_1}$ is the smallest stability region in the set M_c , i.e., $\rho_{low}:=\min\{\rho_i\}$ and $\rho_{e,low}:=\min\{\rho_{e,i}\}$), $i=1,\ldots,|M_c|$). The LEMPC of Eqs. 9-10 is used with an initial model f until it has been decided to modify the process model due to model inaccuracy or

choice of potentially better model structures. At this time, the controller is replaced by Eq. 11 containing a full set of $|M_c|$ mechanistic models. The data-gathering mode can then be activated if desired (assuming that the process state is inside a subset of Ω_{ρ_1} , as will be clarified in Section 3.3) and, thus, the LEMPC selects control actions according to the criteria described above. During the data-gathering process, the set M_c must be adjusted over time by removing/pruning models from the set if certain candidates are found to be inconsistent with the process data. In particular, if the measured state, at any time, exits the stability region of the *i*-th model in M_c , that model is discarded from the set M_c (this is because if the *i*-th mechanistic model structure was accurate to within a bound used in deriving the size of Ω_{ρ_i} , the actual state would be maintained in Ω_{ρ_i} , as will be demonstrated in Section 3.3).

The concept behind the term multiplying β_2 in Eq. 11a is as follows: state measurements will be available over the next sampling period under whichever input is computed by the LEMPC. If one of the mechanistic models in the set is more accurate compared to others (according to a metric such as the norm of the difference between the state prediction at the end of a sampling period under a model and the actual measurement at the next sampling time, which is a similar concept for identifying model correctness as in, for example, 25), this means that the others fail to cause the state trajectory which they compute under a given input to match the actual data obtained from the process under that same input. The one that is sufficiently accurate, under any input selected by the LEMPC, will make predictions that are "close" (according to the metric) to the measurements under the same input. If the same input also causes the less accurate model to make state predictions that are as different as possible from the predictions under the other models (which is the goal in Eq. 11a), then its predictions may be more different from the state predictions from the more accurate model and potentially also from the actual measurements over the next sampling period as well, which can help to flag it as less accurate. Then, though it is not known which model in the set M_c enables predictions to be made to within a desired tolerance of the actual process behavior, the concept of attempting to cause the predictions from the $|M_c|$ models to differ from one another as much as possible in Eq. 11a is due to the recognition that if at least one of the mechanistic models in the set is more accurate compared to others, the inputs that cause the state predictions to differ significantly under different mechanistic models may also cause the actual process data to differ significantly compared to some models. Whenever the metric exceeds a threshold used for discriminating between the more accurate and less accurate mechanistic model candidates (denoted by ϵ_M) for a given model, that model is discarded from M_c . Though the weightings and interactions between terms can complicate these goals of using the term multiplying β_2 in Eq. 11a, and even the standard profit-based objective function of LEMPC may be sufficient for enabling inputs selected to be discriminating, there is potential that the additional term multiplying β_2 could be useful for the data-gathering goals for model discrimination.

An important note in terms of the feasibility of the optimization problem of Eq. 11 is that each of the M_c mechanistic models can have a different steady-state input so that the stabilizing Lyapunov-based controllers $h_{NL,i}$ for each can be different. Therefore, $h_{NL,1}$ does not necessarily drive the actual closedloop state toward a neighborhood of the origin if it or a control action satisfying Eqs. 11f-11g is applied. Therefore, to ensure that a control action that satisfies Eqs. 11f-11g in the case that the i=1 model is not accurate does not drive the closed-loop state out of the stability region of a more accurate model over a sampling period, the stability regions for all models should be nested with Ω_{ρ_i} , i > 1, sufficiently larger than Ω_{ρ_1} such that if the closed-loop state starts in Ω_{ρ_1} , then it cannot leave Ω_{ρ_2} within a sampling period regardless of the input applied (that includes $h_{NL,1}$). This requirement is equivalent to a condition that Ω_{ρ_2} must be sufficiently larger than Ω_{ρ_1} , given the sampling period length and process dynamics (this will be made more precise in Section 3.3). However, because the models are pruned from M_c over time and we do not know a priori which of the mechanistic models is more accurate than others, we do not know if the original i=1 mechanistic model may be discarded. If it is discarded and the original i=2 mechanistic model is not, then the updated set of models is re-numbered (e.g., the original i=2 mechanistic model becomes the updated i = 1 mechanistic model for the next sampling period). In that case, it will be required that the original i=2 mechanistic model has a stability region sufficiently smaller than that of the next model so that when $h_{NL,2}$ is a feasible control action, it cannot drive the closed-loop state out of the next largest stability region. Without loss of generality, we consider that only one of the models will be the most accurate based on the procedure above, and denote the stability region of this more accurate mechanistic model as Ω_{ρ_a} , where $a \in \{1, \ldots, |M_c|\}$. However, it is not known which of the mechanistic models the a-th model corresponds to until the data-gathering is complete.

Remark 1. A particular challenge for designing reliable mechanistic models is introduced when the underlying process dynamics change over time (due to, for example, catalyst deactivation) and, thus, the

model used by the controller without any revision may be less representative of the process and should be revised. Process data recorded off-line or obtained from steady-state operation may not carry meaningful information for the purpose of reidentifying and discriminating between mechanistic models during process operation; an online (control-assisted) selection of the process model after a system identification approach is more suitable for this goal.

Remark 2. In the literature, several EMPC schemes have been proposed for which closed-loop stability can be guaranteed, which, in addition to LEMPC, include EMPC with terminal equality or terminal region constraints,²⁶ with generalized terminal constraints,²⁷ without terminal constraints,²⁸ or robust EMPC methods.^{29,30} We would not expect the ability of EMPC to aid in mechanistic model discrimination to be restricted to LEMPC, but conditions required to achieve safety during mechanistic model discrimination with other control policies are outside the scope of the present work.

Remark 3. The proposed approach could be utilized to attempt to discriminate even between non-mechanistic models; however, since the models in such a case might be derived from data, and the proposed approach gathers data for selecting models, the approach is more applicable if insufficient data was utilized to develop them.

3.2. LEMPC for Discriminating Between Mechanistic Models: Implementation Strategy

Assuming that a reasonably accurate mechanistic model is used by the proposed LEMPC design at the beginning of the process operation, the implementation strategy below includes a region $\rho_{e,low} = \rho_{e,1}$, which is chosen such that if the actual state is in $\Omega_{\rho_{e,low}} \subset \Omega_{\rho_i}$, under sufficient conditions, then the closed-loop state is maintained in Ω_{ρ_i} for $t \geq 0$ if the *i*-th mechanistic model is sufficiently accurate. Particularly, information may be gathered automatically as follows (assuming that $x(t_k) \in \Omega_{\rho_{e,low}}$):

- 1. At the sampling time t_k , the LEMPC of Eq. 11 receives the state measurement $x(t_k)$. If it is desired to optimize economics, set $\beta_1 = 1$. If it is desired to operate the LEMPC in a data-gathering mode (i.e., attempting to maximize differences between state trajectories), set $\beta_2 = 1$, and go to Step 2.
- 2. The LEMPC of Eq. 11 computes control actions that may cause the state trajectories predicted based on the different mechanistic model candidates in M_c to differ from one another under the same input. The computed inputs are applied to the process for a sampling period. Go to Step 3.

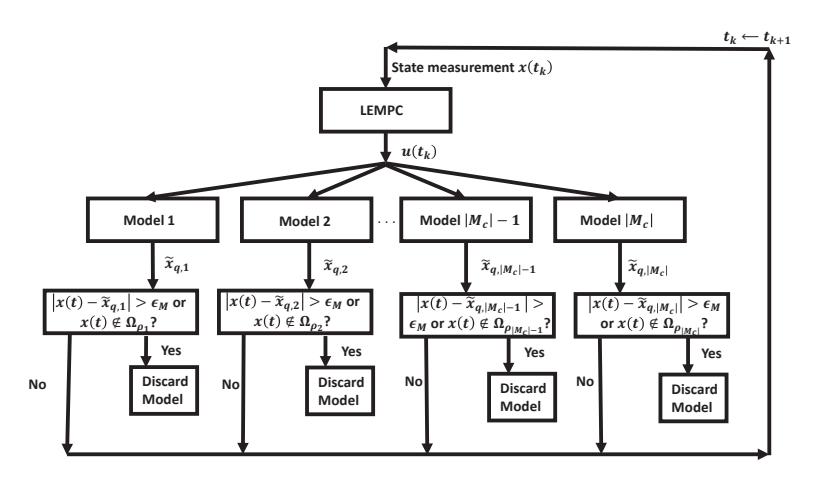


Figure 1: Workflow for checking model accuracy.

- 3. Check the value of x(t), $t \in [t_k, t_{k+1}]$ and the values of the prediction error metrics for each of the mechanistic models in M_c that are to be used for distinguishing between the rival mechanistic models. The *i*-th mechanistic model candidate $(i = 1, 2, ..., |M_c|)$ is discarded from the set M_c if: 1) the prediction error metric evaluated for $\tilde{x}_{q,i}$ (the predicted state using the *i*-th mechanistic model) and the state measurement x is above the accuracy threshold (ϵ_M) ; or 2) the value of x(t), $t \in [t_k, t_{k+1}]$ is outside of the stability region of the *i*-th mechanistic model, $i = 1, 2, ..., |M_c|$. Go to Step 4.
- 4. Go to Step 1 $(k \leftarrow k+1)$.

Fig. 1 shows the major steps in this implementation strategy when models are being discriminated.

Remark 4. To prevent the LEMPC's data-gathering mode from significantly impacting economic optimization, triggering mechanisms may be used. Ideas for these include those which only collect desired information when the optimal solution to the optimization problem is close to the information which it is desired to obtain in a norm sense. For example, the data-gathering mode may be activated when the predicted state of at least one model at the end of a sampling period, $\tilde{x}_{q,i}(t_{k+1})$, is within ϵ_d of a prespecified state, $x_{d,j}$ (e.g., $|\tilde{x}_{q,i}(t_{k+1}) - x_{d,j}| \le \epsilon_d$). A profit-based triggering mechanism may also be used which triggers data-gathering when closed-loop economic performance under the proposed LEMPC with $\beta_2 = 1$ over the next sampling period is within a tolerance ϵ_p of what would be obtained if $\beta_2 = 0$. These types of triggering mechanisms may be particularly beneficial when there is a possibility that the case with $\beta_2 = 0$ may be sufficient for aiding in mechanistic model discrimination, because they allow the profit-based component of the objective function to be "tried" for model discrimination before attempts to gather data

in a non-standard way are made.

3.3. LEMPC for Discriminating Between Mechanistic Models: Stability Analysis

In this section, we prove recursive feasibility and closed-loop stability of the process of Eq. 1 under the implementation strategy of Section 3.2. The impacts of bounded plant/model mismatch on the process state trajectory are delineated in Proposition 1, and Proposition 2 bounds the Lyapunov function value at different points in the stability region.

Proposition 1. ⁵Consider the systems below

$$\dot{x}_a = f(x_a(t), u(t), w(t)) \tag{12a}$$

$$\dot{x}_{b,i} = f_{NL,i}(x_{b,i}(t), u(t) - u_{a,i,s}) \tag{12b}$$

with initial states $x_a(t_0) = x_{b,i}(t_0) \in \Omega_{\rho_i}$ with $t_0 = 0$. There exists a function $f_{W,i}(\cdot)$ such that for $t \in [0,T]$:

$$|x_a(t) - x_{b,i}(t)| \le f_{W,i}(t - t_0) \tag{13}$$

for all $x_a(t), x_{b,i}(t) \in \Omega_{\rho_i} \subset \Omega_{\tilde{\rho}}, u \in U, and w \in W, with$

$$f_{W,i}(\tau) := \left(\frac{L_w \Theta + M_{err,i}}{L_x}\right) e^{(L_x \tau - 1)} \tag{14}$$

where $M_{err,i}$ is defined by the following: $|f(x,u,0) - f_{NL,i}(x,u-u_{q,i,s})| \leq M_{err,i}, \ \forall x \in \Omega_{\rho_i} \ and \ u \in U$.

Proposition 2. ³¹ Consider the Lyapunov function $\hat{V}_i(\cdot)$ of the system of Eq. 3 under the controller $h_{NL,i}(\cdot)$ that satisfies Eqs. 4a-4d. There exists a quadratic function $f_{V,i}(\cdot)$ such that:

$$\hat{V}_i(\bar{x}) \le \hat{V}_i(\bar{x}') + f_{V,i}(|\bar{x} - \bar{x}'|) \tag{15}$$

for all $\bar{x}, \bar{x}' \in \Omega_{\rho_i}$ with

$$f_{V,i}(s) := \hat{\alpha}_{4,i}(\hat{\alpha}_{1,i}^{-1}(\rho_i))s + M_{v,i}s^2$$
(16)

where $M_{v,i}$ is a positive constant.

The following theorem guarantees closed-loop stability of the process of Eq. 1 under the implementation strategy of Section 3.2.

Theorem 1. Consider the closed-loop system of Eq. 1 under the implementation strategy of Section 3.2, where $h_{NL,i}(\cdot)$ used in the LEMPC of Eq. 11 for any i-th model in the set M_c meets the inequalities in Eqs. 4a-4d with respect to the i-th model candidate. Let $\epsilon_{W_i} > 0$, $\Delta > 0$, and $N \ge 1$. At every sampling time, let $\Omega_{\rho_{low}} \subseteq \Omega_{\rho_i} \subset X$, where $\rho_{low} := \min\{\rho_i\}$ and $\rho_{e,low} := \min\{\rho_{e,i}\}$ for the models which are in the set M_c at a sampling time. Also, assume that:

$$\left| \frac{\partial \hat{V}_a(x(t))}{\partial x} - \frac{\partial V(x(t))}{\partial x} \right| \le M_g \tag{17}$$

where $M_g > 0$, for all $x \in \Omega_{\tilde{\rho}}$. Let $\rho_{e,i} > \rho_{\min,i} > \rho_{s,i}$, $\rho_i > \rho_{e,i} > \rho_{i-1}$, for $i = 1, 2, \ldots, |M_c|$, satisfy:

$$-\hat{\alpha}_{3,i}(\hat{\alpha}_{2,i}^{-1}(\rho_{s,i})) + \hat{L}'_{x,i}\hat{M}_{fi}\Delta \le -\epsilon_{w,i}/\Delta, \ i = 1, \dots, |M_c|$$
(18)

$$-\hat{\alpha}_{3,a}(\hat{\alpha}_{2,a}^{-1}(\rho_{e,a})) + \hat{\alpha}_{4,a}(\hat{\alpha}_{1,a}^{-1}(\rho_a))M_{err,a} + L_x'M_f\Delta + L_w'\Theta + 2M_gM_f \le -\epsilon_{w,a}'\Delta$$
(19)

$$\rho_{e,a} + f_{V,a}(f_{W,a}(\Delta)) \le \rho_a \tag{20}$$

$$\rho_{e,i} \ge \max\{\hat{V}_i(x(t)) : x(t_k) \in \Omega_{\rho_{i-1}}, t \in [t_k, t_{k+1}), u \in U, w \in W\}, i = 2, \dots, |M_c|$$
(21)

$$\rho_{\min,i} \ge \max\{\hat{V}_i(x(t)) : x(t_k) \in \Omega_{\rho_{s,i}}, t \in [t_k, t_{k+1}), u \in U, w \in W\}, i = 1, \dots, |M_c|$$
(22)

$$\rho_{\min,i} \ge \max\{\hat{V}_i(\tilde{x}_{q,i}(t)) : \tilde{x}_{q,i}(t_k) \in \Omega_{\rho_{s,i}}, t \in [t_k, t_{k+1}), u \in U, w \in W\}, i = 1, \dots, |M_c|$$
(23)

If $x(t_0) \in \Omega_{\rho_{e,1}}$ for the i = 1 model in the set M_c at t_0 , then $x(t) \in \Omega_{\rho_a}$ for $t \ge 0$.

Proof. The proof consists of two parts. In the first part, recursive feasibility at every sampling time under the implementation strategy of Section 3.2 is demonstrated. In the second part, it is demonstrated that the closed-loop state is maintained within Ω_{ρ_a} for all times (regardless of whether $\beta_p = 0$ or $\beta_p = 1$, p = 1, 2) if $x(t_0) \in \Omega_{\rho_{e,1}} = \Omega_{\rho_{e,low}}$ at t_0 .

Part 1. We first demonstrate that $h_{NL,1}$ is a feasible solution to the LEMPC of Eq. 11, with either $\beta_p = 0$ or $\beta_p = 1$, p = 1, 2, at all sampling times under the implementation strategy of Section 3.2. Under this implementation strategy, at time t_0 , $h_{NL,1}$ satisfies the constraint of Eq. 11e from Eq. 4d with respect to the i = 1 model. It also satisfies Eqs. 11f-11g.²³ Specifically, the system state $\tilde{x}_{q,i}(t_0)$ must be inside the smallest stability region $\rho_{e,low} \subset \rho_{low}$. In this case, $h_{NL,1}(\cdot)$ implemented in sample-and-hold is a feasible input policy because it trivially satisfies Eq. 11g. Furthermore, under the conditions in Eqs. 18

and 23, $h_{NL,1}$ satisfies Eq. 11f if $\tilde{x}_{q,i}(t_0) = x(t_0) \in \Omega_{\rho_{e,low}} \subseteq \Omega_{\rho_{low}}$ (and thereby Eq. 11d since $\Omega_{\rho_{low}} \subset X$). Specifically, from Eq. 4b, if $\tilde{x}_{q,i}(t_k) \in \Omega_{\rho_1}/\Omega_{\rho_{s,1}}$, where $\rho_1 = \rho_{low}$:

$$\frac{\partial \hat{V}_1(\tilde{x}_{q,1}(t_p))}{\partial \tilde{x}_{q,1}} f_{NL,1}(\tilde{x}_{q,1}(t_p), h_{NL,1}(\tilde{x}_{q,1}(t_p))) \le -\hat{\alpha}_{3,1}(|\tilde{x}_{q,1}(t_p)|), \ p = k, \dots, k + N - 1$$
 (24)

Therefore, for $t \in [t_p, t_{p+1})$ and $p = k, \dots, k+N-1$ and $\tilde{x}_{q,1}(t_p) \in \Omega_{\rho_1}/\Omega_{\rho_{s,1}}$:

$$\frac{\partial \hat{V}_{1}(\tilde{x}_{q,1}(t))}{\partial \tilde{x}_{q,1}} f_{NL,1}(\tilde{x}_{q,1}(t), h_{NL,1}(\tilde{x}_{q,1}(t_{p}))) \le -\hat{\alpha}_{3,1}(\hat{\alpha}_{2,1}^{-1}(\rho_{s,1})) + \hat{L}'_{x,1}\hat{M}_{f_{1}}\Delta$$
(25)

where this inequality follows from adding and subtracting $\frac{\partial \hat{V}_1(\tilde{x}_{q,1}(t_p))}{\partial \tilde{x}_{q,1}}$ $f_{NL,1}(\tilde{x}_{q,1}(t_p), h_{NL,1}(\tilde{x}_{q,1}(t_p)))$ to/from $\frac{\partial \hat{V}_1(\tilde{x}_{q,1}(t))}{\partial \tilde{x}_{q,1}}$ $f_{NL,1}(\tilde{x}_{q,1}(t), h_{NL,1}(\tilde{x}_{q,1}(t_p)))$ and applying the triangle inequality, and subsequently using Eqs. 4a, 5a, and 6. If Eq. 18 holds, $\frac{\partial \hat{V}_1(\tilde{x}_{q,1}(t))}{\partial \tilde{x}_{q,1}}$ $f_{NL,1}(\tilde{x}_{q,1}(t), h_{NL,1}(\tilde{x}_{q,1}(t_p)))$ is negative with $\hat{V}_1(t) \leq \hat{V}_1(t_p)$ for $t \in [t_p, t_{p+1})$ so that if $\tilde{x}_{q,1}(t_p) \in \Omega_{\rho_{e,low}} \subseteq \Omega_{\rho_{low}}$, then $\tilde{x}_{q,1}(t) \in \Omega_{\rho_{e,low}}$, $\forall t \in [t_p, t_{p+1})$. If instead $\tilde{x}_{q,1}(t_p) \in \Omega_{\rho_{s,1}}$, then from Eq. 23 and $\rho_{e,low} > \rho_{\min,1} > \rho_{s,1}$, $\tilde{x}_{q,1}(t) \in \Omega_{\rho_{\min,1}} \subset \Omega_{\rho_{e,low}} \subseteq \Omega_{\rho_{low}}$ for $t \in [t_p, t_{p+1})$, as required by the constraint of Eq. 11f.

At time t_1 , the closed-loop state is in Ω_{ρ_a} , as will be demonstrated below. In this case, one of two outcomes occurred at t_1 according to the implementation strategy in Section 3.2: 1) models were removed from M_c ; 2) models were not removed from M_c . If no models were removed, the original i=1 model is still the model corresponding to $\Omega_{\rho_{low}}$. In that case, the closed-loop state is again in $\Omega_{\rho_{low}}$, and feasibility will again hold by the proof above. If models were removed from M_c , the remaining models are re-numbered so that the model with the smallest stability region is labeled as the i=1 model, that with the next largest stability region is labeled as the i=2 model, and so forth. At this sampling time, $x(t_k) \in \Omega_{\rho_1}$ for the new i=1 model (or else that model would have been discarded according to the implementation strategy of Section 3.2), and the new $h_{NL,1}$ again satisfies Eqs. 11e, 11d, 11f, and 11g from the proof above. Applying these arguments recursively indicates that the $h_{NL,1}$ for the current set of $i=1,\ldots,|M_c|$ models at any sampling time is a feasible solution to Eq. 11. Thus, there is a feasible solution to Eq. 11 at every sampling time when the implementation strategy in Section 3.2 is used.

Part 2. We now demonstrate that under the implementation strategy in Section 3.2, the closed-loop state is maintained within Ω_{ρ_a} for all times. At t_0 , $x(t_0) \in \Omega_{\rho_{e,low}} \subset \Omega_{\rho_a}$. Eq. 11 ensures that $\hat{V}_1(\tilde{x}_{q,1}(t)) \leq \rho_{e,1}$. Either the i=1 model corresponds to i=a, or a model with i>1 corresponds to i=a. If i>1

corresponds to i=a, then Eq. 21 ensures that $x(t) \in \Omega_{\rho_a}$, $t \in [t_k, t_{k+1})$ since $x(t_k) \in \Omega_{\rho_1}$. If i=1 corresponds to i=a, then from Propositions 1 and 2:

$$\hat{V}_a(x(t)) \le \hat{V}_a(\tilde{x}_{q,a}(t)) + f_{V,a}(|\tilde{x}_{q,a}(t) - x(t)|) \le \rho_{e,a} + f_{V,a}(f_{W,a}(\Delta))$$
(26)

for $t \in [t_0, t_1)$. If Eq. 20 holds, then $x(t) \in \Omega_{\rho_a}$ for $t \in [t_0, t_1)$. At t_1 , either models are removed from the set M_c according to the implementation strategy in Section 3.2, or they are not. In either case, the new value of ρ_{low} either is the same as ρ_a (it cannot be greater because the i=a model will not be discarded if the prediction error metric threshold is set to avoid removing sufficiently accurate models from M_c and if $x(t) \in \Omega_{\rho_a}$, $t \in [t_0, t_1)$ (which was proven to hold when Eqs. 21 and 20 hold) so that the model cannot be removed for the closed-loop state leaving Ω_{ρ_a}) or less than ρ_a at t_1 . In either case, the closed-loop state is in the updated $\Omega_{\rho_{low}} \subseteq \Omega_{\rho_a}$. In this case, either $x(t_k) \in \Omega_{\rho_{low}}/\Omega_{\rho_{e,low}}$ or $x(t_k) \in \Omega_{\rho_{e,low}}$. If $x(t_k) \in \Omega_{\rho_{e,low}}$, then the constraint of Eq. 11f holds for the i=1 model, and again Eq. 21 and Eq. 20 ensure that $x(t) \in \Omega_{\rho_a}$, $t \in [t_1, t_2)$, whether the i=1 model corresponds to i=a or a model with i>1 corresponds to i=a.

If instead $x(t_k) \in \Omega_{\rho_{low}}/\Omega_{\rho_{e,low}}$, then the constraint of Eq. 11g is activated. If i > 1 corresponds to the i = a model, then Eq. 21 ensures that $x(t) \in \Omega_{\rho_a}$ for $t \in [t_k, t_{k+1})$. If instead i = 1 corresponds to i = a, then Eq. 24 holds for the i = 1 model with $h_{NL,1}(\tilde{x}_{q,1}(t_p))$ replaced by $u_{q,1}(t_p)$. A bound on the time derivative of the Lyapunov function at t_1 for the nominal model of Eq. 1 under $u(t_1) = u_{q,1}(t_1) + u_{q,1,s}$ can be developed as follows:

$$\frac{\partial \hat{V}_1(x(t_1))}{\partial x} f(x(t_1), u(t_1), 0) \le -\hat{\alpha}_{3,1}(|x(t_1)|) + \hat{\alpha}_{4,1}(|x(t_1)|) M_{err,1}$$
(27)

which is derived from adding and subtracting $\frac{\partial \hat{V}_1(x(t_1))}{\partial x} f_{NL,1}(x(t_1), u(t_1) - u_{q,1,s})$ to/from $\frac{\partial \hat{V}_1(x(t_1))}{\partial x} f(x(t_1), u(t_1), 0)$, and applying Eq. 4c, Eq. 24, and the definition of $M_{err,i}$. $\dot{\hat{V}}_1$ along the

closed-loop state trajectory under $u(t_1)$ is then obtained from:

$$\frac{\partial \hat{V}_{1}(x(t))}{\partial x} f(x(t), u(t_{1}), w(t)) \leq \frac{\partial \hat{V}_{1}(x(t))}{\partial x} f(x(t), u(t_{1}), w(t)) - \frac{\partial V(x(t))}{\partial x} f(x(t), u(t_{1}), w(t)) + \frac{\partial V(x(t))}{\partial x} f(x(t), u(t_{1}), w(t)) - \frac{\partial V(x(t_{1}))}{\partial x} f(x(t_{1}), u(t_{1}), 0) + \frac{\partial V(x(t_{1}))}{\partial x} f(x(t_{1}), u(t_{1}), 0) - \frac{\partial \hat{V}_{1}(x(t_{1}))}{\partial x} f(x(t_{1}), u(t_{1}), 0) + \frac{\partial \hat{V}_{1}(x(t_{1}))}{\partial x} f(x(t_{1}), u(t_{1}), 0)$$

$$\leq \left| \frac{\partial \hat{V}_{1}(x(t))}{\partial x} - \frac{\partial V(x(t))}{\partial x} \right| |f(x(t), u(t_{1}), w(t))| + L'_{x}|x(t) - x(t_{1})| + L'_{w}|w| + \frac{\partial V(x(t_{1}))}{\partial x} - \frac{\partial \hat{V}_{1}(x(t_{1}))}{\partial x} |f(x(t_{1}), u(t_{1}), w(t_{1}))| - \hat{\alpha}_{3,1}(|x(t_{1})|) + \hat{\alpha}_{4,1}(|x(t_{1})|) M_{err,1}$$

$$\leq -\hat{\alpha}_{3,1}(|x(t_{1})|) + \hat{\alpha}_{4,1}(|x(t_{1})|) M_{err,1} + 2M_{g}M_{f} + L'_{x}M_{f}\Delta + L'_{w}\Theta$$

$$\leq -\hat{\alpha}_{3,a}(\hat{\alpha}_{2,a}^{-1}(\rho_{e,a})) + \hat{\alpha}_{4,a}(\hat{\alpha}_{1,a}^{-1}(\rho_{a})) M_{err,a} + L'_{x}M_{f}\Delta + L'_{w}\Theta + 2M_{g}M_{f}$$
(28)

which is obtained from applying the triangle inequality, Eqs. 4a, 7b, 8, 17, and 27, continuity of x, the fact that $x(t_1) \in \Omega_{\rho_a}/\Omega_{\rho_{e,a}}$, and the bound on w. When Eq. 19 holds, Eq. 28 implies that the value of \hat{V}_1 is decreasing over time along the closed-loop state trajectory, so that $\hat{V}_1(x(t)) \leq \hat{V}_1(x(t_1)) \leq \rho_a$ for $t \in [t_1, t_2)$. Applying this recursively, the actual state stays within Ω_{ρ_a} at all times.

Remark 5. When the conditions of Theorem 1 hold, bounded plant/model mismatch with magnitudes Θ and $M_{err,a}$ enable closed-loop stability to be guaranteed under the a-th model (i.e., every model for which bounds on the plant/model mismatch meet the conditions of Theorem 1, along with the other functions and parameters used in LEMPC, is considered to be "sufficiently accurate" because it maintains system safety). Therefore, from Proposition 1, $|x_{q,a}(t_k) - \tilde{x}_{q,a}(t_k|t_{k-1})| \leq f_{W,a}(\Delta)$, where $\tilde{x}_{q,a}(t_k|t_{k-1})$ is the predicted state at t_k using the a-th model initialized from the state measurement at t_{k-1} . Although the accurate model is unknown, the value $f_{W,a}(\Delta)$ represents that there exists a lower bound on the threshold ϵ_M that avoids flagging a sufficiently accurate model as inaccurate due to the presence of disturbances, but without allowing excessive amounts of model error. If ϵ_M is greater than $f_{W,a}(\Delta)$, the detection threshold avoids flagging acceptable plant/model mismatch as unacceptable (i.e., it would avoid pruning a sufficiently accurate model from M_c). However, which models are sufficiently accurate for maintaining closed-loop stability under LEMPC is not known a priori so that less accurate models may also fall within

a given bound ϵ_M on the prediction error, or the bound on the prediction error might be set too low in practice so that a sufficiently accurate model is pruned. Other metrics besides prediction error could also be considered for evaluating whether models should remain within M_c or not.

Remark 6. Another way to implement the proposed control design and prove closed-loop stability for all time is to enforce the constraint of Eq. 11f not only for the model that corresponds to the smallest stability region but also for each *i*-th model in the set M_c . The proof would follow as above, except that feasibility of each of these added constraints depends on Eq. 21. Although models are discarded from M_c during the data-gathering process, which progressively reduces the number of constraints enforced on this alternative control design over time, this control implementation is not as streamlined as that in Section 3.1 in the sense that as the number of models $|M_c|$ grows, more constraints are imposed on the closed-loop state.

Remark 7. The results of Theorem 1 hold assuming that a model for which the plant/model mismatch is sufficiently small (in the sense that the conditions of the theorem hold for the model with i=a) is in the set M_c , and that nested stability regions for all candidate models can be found. If it is not possible to nest the stability regions of all possible mechanistic models, the set M_c can be broken up into multiple sets of mechanistic model candidates for which it is possible to nest the stability regions, and then the models in each set can be discriminated following the conditions in Theorem 1 by using the proposed LEMPC for a given set at a time. There would need to be overlap of the different sets or multiple sufficiently accurate models in this case, as the assumption that there is at least one mechanistic model meeting the assumptions of Theorem 1 in the controller used for each set must continue to hold. The assumptions of nested stability regions could be challenging to implement in practice (e.g., to meet Eq. 21, small values of Δ may be needed, especially if there are many possible models that must be needed); in general, designing LEMPC's that fully meet theoretical conditions for practical use can be a challenge. The potential conservatism and limitations that nesting stability regions might introduce is partially due to a lack of knowledge and lack of a priori data for discriminating between the models before the controller is put online. In general for LEMPC, it may be desirable to use large stability regions. One could attempt to more rigorously determine the region of attraction and use this in evaluating a variety of stability regions to seek to select one which takes up as large a fraction of the region of attraction as possible (e.g., 32,33,34). In practice, one may not know whether a model meeting the requirements of Theorem 1 is in the set; in this case, sufficient data on

process behavior and physics may be necessary to provide a reasonable set of models which is expected to include a model for which the requirements of Theorem 1 hold, or many models might be suggested (i.e., $|M_c|$ might be large) to attempt to include many possible models with the hope that one might meet the requirements of Theorem 1 even if it is not known at the beginning of the model discrimination procedure which it is. It may be challenging to check whether the conditions of Theorem 1 are satisfied when putting an LEMPC online, as some of the conditions (e.g., Eqs. 19 and 20) are required to hold for the sufficiently accurate model but may not hold for the others, and a sufficiently accurate model is not known a priori. Remark 8. It may be possible that more than one model in M_c may be consistent with the available data over time, particularly considering measurement noise and plant/model mismatch between all models and the process dynamics, such that it may not be possible to confidently state that one of the models is better than the other. In such a case, if the conditions of Theorem 1 are satisfied with at least one of the models selected as the a-th model, then one of those that meets the requirements may be selected as the i=amodel, and the system can be run safely (i.e., the closed-loop state will be maintained within Ω_{ρ}). This does not necessarily mean, however, that the mechanisms conveyed by the mechanistic model selected in such a case are those which actually describe the process physics. Because this strategy may combine first-principles modeling (in the development of the mechanistic models) with data (for discriminating between the potential mechanisms suggested), one might consider it an alternative concept of combining first-principles and data-driven techniques in modeling (where certain techniques for doing this often fall

Remark 9. The reason for including both Eqs. 22 and 23 is that the latter is needed to ensure that the state predictions do not leave $\Omega_{\rho_{e,i}}$ if $\tilde{x}_{q,i} \in \Omega_{\rho_{e,i}}/\Omega_{\rho_{s,i}}$ (to ensure feasibility of Eq. 11 with the state predictions), whereas Eq. 22 is required for ensuring that the actual closed-loop state does not exit Ω_{ρ_a} .

within a category of "hybrid modeling").

4. EMPC for Discriminating Between Mechanistic Models: Illustrative Process Example

In this section, we provide simulations that illustrate and elucidate some of the concepts discussed above and serve to indicate some of the potential benefits and limitations of using EMPC for model discrimination. This example makes no attempt to fully demonstrate the control theory above, and thus does not rigorously demonstrate the implementation strategy in Section 3.2. Rather, it is intended to showcase more practical

considerations regarding when and how the flexibility of EMPC might be used for model discrimination, to elucidate relevant aspects that were not highlighted in the theory introduced so far, and to provide some discussion toward future automation of digital twin development via control-assisted approaches for gaining non-standard operating data for on-line model development. Exploring how to develop parameters and evaluate the practicality of the method described in Section 3 when full control theory is applied can be a subject of future work, but that theory is important for this discussion in demonstrating that there would be conditions under which safe model discrimination could be performed via control-assisted methods.

For this example, we consider the problem of seeking to, on-line, develop insights into the physics of a process as an initial step toward automated control-assisted digital twin development (and the potential benefits that that might entail for applications such as fault diagnosis, process monitoring, and developing more economically-optimal control strategies). This goal is considered for a non-ideal continuous stirred tank reactor (CSTR) with dead space and bypass, in which a second-order, exothermic, irreversible reaction of the form $A \to B$ is occurring. The dynamics of this system are considered to be represented by a perturbed version of the following dynamic equations (where the perturbations are random numbers from a bounded standard normal distribution that are added to the right-hand side of each of the following equations):

$$\frac{dC_{Am}}{dt} = \frac{F_m}{V_m} (C_{A0} - C_{Am}) - k_0 e^{\frac{-E_0}{RT_m}} C_{Am}^2$$
(29a)

$$C_A = \frac{F_0 - F_m}{F_0} C_{A0} + \frac{F_m}{F_0} C_{Am}$$
 (29b)

$$\frac{dT_m}{dt} = \frac{F_m}{V_m} (T_0 - T_m) + \frac{-\Delta H}{\rho_L C_p} k_0 e^{\frac{-E_0}{RT_m}} C_{A_m}^2 + \frac{Q}{\rho_L C_p V_m}$$
(29c)

$$T = \frac{F_m(T_m - T_0) + F_0 T_0}{F_0} \tag{29d}$$

This non-ideal CSTR has a well-mixed volume V_m , and a total volume V. The concentration of species A, volumetric flow rate, and temperature in this well-mixed part of the reactor are denoted as C_{Am} , F_m , and T_m respectively. This reactor also presents a dead zone (with volume $V - V_m$) and a bypass (with a volumetric flow rate of $F_0 - F_m$). To complete the model for the actual process dynamics, process disturbances were added to the right-hand side of the differential equations describing the rates of change of C_A and T with zero mean and standard deviations of 20 kmol/m³ h and 100 K/h, and bounds of 10 kmol/m³ h and 50 K/h, respectively. Measurement noise was also included based on a standard normal distribution with mean zero, standard deviations of 0.01 kmol/m³ and 1 K, and bounds of 0.05 kmol/m³ and 5 K for the

concentration of the reactant and reactor temperature, respectively. The process parameters are presented in Table 1. The steady-state values of the states C_{Am} and T_m and inputs are $C_{Ams} = 1.22 \text{ kmol/m}^3$, $T_{ms} = 438.2 \text{ K}$, $C_{A0s} = 3.888 \text{ kmol/m}^3$, and $Q_s = 6.387 \times 10^3 \text{ kJ/h}$, respectively. The vectors of deviation variables for the states and inputs from their steady-states are $x = [x_1 \ x_2]^T = [C_A - C_{As} \ T - T_s]^T$ and $u = [u_1 \ u_2]^T = [C_{A0} - C_{A0s} \ Q - Q_s]^T$. It is assumed that the sensors for concentration and temperature of the reactor are placed within the well-mixed part of the reactor and that the process has been operated at the steady-state in the past, so that most of the available process data consists of measurements reading C_{Ams} and T_{ms} . We also assume that the controller readings $(C_{A0s} \ \text{and} \ Q_s)$ are available. However, though F_0 is assumed to be fixed and measurable, T_0 is not measured. Also, there is no sensor for potential impurities in the feed that could impact reaction kinetics. The total reactor volume is assumed to be monitored via a level sensor, so that V is also known.

Table 1: Parameters for the CSTR models.

Parameter	${f Value}$	\mathbf{Unit}	
\overline{V}	1	m^3	
$\overline{T_0}$	300	K	
C_p	0.231	${ m kJ/kg\cdot K}$	
k_0	8.46×10^{6}	$\mathrm{m^3/h \cdot kmol}$	
F_0	5	$ m m^3/h$	
$ ho_L$	1000	${ m kg/m^3}$	
$\overline{E_0}$	5×10^4	${ m kJ/kmol}$	
R	8.314	${ m kJ/kmol\cdot K}$	
ΔH	-1.15×10^4	${ m kJ/kmol}$	
$\overline{F_m}$	$0.99F_0$	$ m m^3/h$	
V_m	0.95V	m^3	
$\overline{F_{m1}}$	4.95	$ m m^3/h$	
E_{01}	5.019×10^4	kJ/kmol	
V_{m3}	0.9596	m^3	
T_{03}	300.06	K	

It is assumed that the plant engineers would like to enhance the profitability of the process by obtaining a more accurate model of the process dynamics to aid in operating the process under EMPC and also to aid with process monitoring efforts. To do this, a control-assisted approach will be used that is similar in concept to that described in Section 3 (though without being rigorously designed to meet all control-theoretic conditions needed for guaranteeing safety during the data-gathering process). Specifically, a set of

rival mechanistic models will be identified where the available data for discrimination between these models is insufficient for selecting which is the most accurate because most of the available dataset was developed when operating at a steady-state, and the data from dynamic operation is limited. We desire to use EMPC to aid in discriminating between the rival mechanistic model candidates online. Particularly, the control objective is to select a suitable mechanistic model candidate within the set M_c to be used by the controller.

The first question to be addressed is which models will be in the set M_c . We consider that the plant engineers have hypothesized that the reactor may have bypass and dead zone, but that they do not know if it has both or only one of these non-ideal scenarios. Therefore, the model structures for the mechanistic models consider that both dead zone and bypass may occur (as in Eq. 29), that only dead zone may occur, or that only bypass may occur. However, though this fixes several potential model structures, it does not fix their parameters, and the strategy presented in Section 3 for control-assisted model structure selection requires that the model parameters already be identified or postulated for every model in M_c . We note, however, that because some operating data is available (primarily at steady-state) and some data on the physical process is available (e.g., knowledge of V), it is not possible for all possible model parameters to be valid. Consider, for example, a model structure of the following form, representing a system with bypass only (with a bypass flow rate of $F_0 - \bar{F}_m$):

$$\frac{dC_{Am}}{dt} = \frac{\bar{F}_m}{V}(C_{A0} - C_{Am}) - \bar{k}_0 e^{\frac{-\bar{E}_0}{RT_m}} C_{Am}^2$$
(30a)

$$C_A = \frac{F_0 - \bar{F}_m}{F_0} C_{A0} + \frac{\bar{F}_m}{F_0} C_{Am} \tag{30b}$$

$$\frac{dT_m}{dt} = \frac{\bar{F}_m}{V}(\bar{T}_0 - T_m) + \frac{-\Delta H}{\rho_L C_p} \bar{k}_0 e^{\frac{-\bar{E}_0}{RT_m}} C_{A_m}^2 + \frac{Q}{\rho_L C_p V}$$
(30c)

$$T = \frac{\bar{F}_m(T_m - \bar{T}_0) + F_0\bar{T}_0}{F_0}$$
(30d)

In these equations, \bar{F}_m , \bar{T}_0 , \bar{k}_0 , and \bar{E}_0 (the bypass flow rate, feed temperature, pre-exponential factor, and activation energy) are considered to be parameters that, based on the sensing/monitoring setup in place for this process described above, could be values different from what is expected. However, because we know that when $C_{Ams} = 1.22 \text{ kmol/m}^3$ and $T_{ms} = 438.2 \text{ K}$, then $C_{A0s} = 3.888 \text{ kmol/m}^3$ and $Q_s = 6.387 \times 10^3 \text{ kJ/h}$, we can attempt to check whether different values of the unknown parameters are consistent with the steady-state data. For example, consider the case where $\bar{k}_0 = k_0$ and $\bar{E}_0 = E_0$ in Table 1 (i.e., only \bar{F}_m and \bar{T}_0 are considered to be unknown). In this case, values of \bar{F}_m and \bar{T}_0 that satisfy the steady-

state form of Eq. 30 when $C_{Am} = C_{Ams}$, $T_m = T_{ms}$, $C_{A0} = C_{A0s}$, and $Q = Q_s$, obtained using fsolve in MATLAB R2016b with an initial guess of $\bar{F}_m = 5 \text{ m}^3/\text{h}$ and $\bar{T}_0 = 300 \text{ K}$, are $\bar{F}_m = 5.21 \text{ m}^3/\text{h}$ and $\bar{T}_0 = 300.3 \text{ K}$. However, we would discard these potential values of the parameters because though they are consistent with the steady-state data, they are not consistent with our knowledge that F_0 is 5 m³/h, so that the maximum possible value of the bypass flow rate (which is a fraction of this) must be less than 5 m³/h. This demonstrates that even with limited data available, the physics of the system can set bounds on potential allowable values of parameters in potential mechanistic model structures based on different physics postulates, aiding in forming the set M_c .

For the purposes of illustration, we will utilize a limited set of models (only three mechanistic model candidates) in the remainder of this example, though more could be developed. One is the mechanistic model of Eq. 29 (which is close to the "actual" process dynamics but still differs from these dynamics because there are disturbances added to the right-hand side of Eq. 29 for the "actual" process), one is a mechanistic model assuming only a dead zone in the reactor (no bypass), and one is a mechanistic model assuming only bypass through the reactor (and no dead zone). All three consider the second-order, exothermic, irreversible reaction $(A \to B)$ to be occurring in the CSTR. Based on attempts like that described in the prior paragraph to obtain model candidates for which there is a steady-state with the measured values of concentration and temperature in any well-mixed portion of a reactor set to C_{Ams} and T_{ms} when $C_{A0} = C_{A0s}$ and $Q = Q_s$, parameters for the dead space and bypass flow rates, as well as some kinetics and feed data, are different between the models. Fig. 2 illustrates the different physics considered for the three model candidates. Below, the three mechanistic model candidates are numbered/ordered for use in an EMPC with a similar form to that in Eq. 11.

The first mechanistic model candidate (Model 1; i = 1 in the original set M_c), which is represented by Fig. 2a, is a non-ideal CSTR with bypass ($F_b = F_0 - F_{m1}$), but without considering dead space, and can be described by the following equations:

$$\frac{dC_{Am}}{dt} = \frac{F_{m1}}{V}(C_{A0} - C_{Am}) - k_0 e^{\frac{-E_{01}}{RT_m}} C_{Am}^2$$
(31a)

$$C_A = \frac{F_0 - F_{m1}}{F_0} C_{A0} + \frac{F_{m1}}{F_0} C_{Am} \tag{31b}$$

$$\frac{dT_m}{dt} = \frac{F_{m1}}{V}(T_0 - T_m) + \frac{-\Delta H}{\rho_L C_p} k_0 e^{\frac{-E_{01}}{RT_m}} C_{A_m}^2 + \frac{Q}{\rho_L C_p V}$$
(31c)

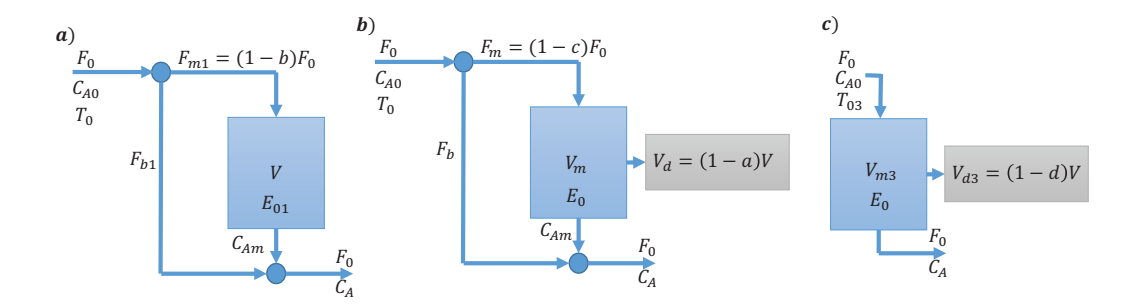


Figure 2: Mechanistic CSTR model candidates (a) has only bypass, (b) has bypass and a dead zone, and (c) has only a dead zone. For the model candidate in (a), F_{m1} represents the volumetric flow rate into and out of the well-mixed portion of the CSTR, and F_{b1} represents the bypass flow rate (which is a fraction b of the inlet volumetric flow rate F_0). For the model candidate in (b), F_m represents the volumetric flow rate into and out of the well-mixed portion of the CSTR, which is a fraction (1-c) of the total volumetric flow rate F_0 into the CSTR (the fraction c of the total volumetric flow rate is F_b). V_d represents the volume of the dead zone, which is a fraction c of c (the fraction c) of the total volume is the well-mixed part c). For the model candidate in (c), the dead zone c0 is a fraction c0 of the total volume, with c1 representing the volume of the well-mixed part of the CSTR.

$$T = \frac{F_{m1}(T_m - T_0) + F_0 T_0}{F_0} \tag{31d}$$

The second mechanistic model candidate (Model 2; i = 2 in the original set M_c) is represented by Fig. 2b and has the dynamics in Eq. 29. The third mechanistic model candidate (Model 3; i = 3 in the original set M_c), which is represented by Fig. 2c, is a non-ideal CSTR with dead space ($V = V_d + V_{m3}$), but without considering bypass, and can be described by the equations below:

$$\frac{dC_A}{dt} = \frac{F_0}{V_{m3}} (C_{A0} - C_A) - k_0 e^{\frac{-E_0}{RT}} C_A^2$$
(32a)

$$\frac{dT}{dt} = \frac{F_0}{V_{m3}}(T_{03} - T) + \frac{-\Delta H}{\rho_L C_p} k_0 e^{\frac{-E_0}{RT}} C_A^2 + \frac{Q}{\rho_L C_p V_{m3}}$$
(32b)

The parameters of the three mechanistic model candidates described above are shown in Table 1. All three process models, and the actual plant dynamics, are numerically integrated using the explicit Euler method with an integration step size of 10^{-4} h. We note that because C_A and T differ in the three mechanistic model candidates, the sensor placement in this case makes the discrimination challenging with the steady-state operating data (if, for example, the sensor was placed at the outlet stream of the reactors (i.e., C_A and T were obtained for every case in Fig. 2), a difference may be observed between the expected measurements from the three models when the steady-state inputs are applied, and the models could be discriminated while operating at steady-state).

The EMPC formulation to be used for control-assisted online model discrimination will have a form

similar to that in Eq. 11 (though the constraints will not be designed to meet the control-theoretic conditions). Therefore, it is necessary to design operating regions for the different models to use in constructing the constraints. To do this, a Lyapunov function $\hat{V}_1 = x_{q,i}^T P x_{q,i}$, i = 1, 2, 3, where $P = [1200 \ 5; 5 \ 0.1]$, was selected. To nest the stability regions, the stability region using Model 1 was set to $\rho_1 = 300$ (i.e., $\Omega_{\rho_1} = \{x \in R^2 : \hat{V}_1(x) \le \rho_1\}$) with $\rho_{e,1} = 275$; the stability region using Model 2 was set to $\rho_2 = 370$ with $\rho_{e,2} = 325$; and the stability region using Model 3 was set to $\rho_3 = 470$ with $\rho_{e,3} = 380$. We note that in general, nesting of stability regions may not imply that the models with the larger stability regions can stabilize the closed-loop system under a Lyapunov-based controller from a larger portion of state-space, but rather that a more conservative subset of that region is selected for one of the regions than might otherwise be chosen to facilitate the nesting. However, it makes sense to place stability regions that are more conservative due to the region of state-space from which a given model can be stabilized within stability regions corresponding to models that can be stabilized from a larger region of state-space, to avoid excessive conservatism in the stability region design.

A practical consideration for control-assisted model discrimination is that there need to be subsets of the stability regions where at least some models give sufficiently different state predictions from one another so that some will be able to be pruned from M_c . It is possible to check if this is a possibility using an a priori analysis of the model candidates to see if there are possible initial conditions within the smallest stability region and inputs within the input bounds which can maintain the closed-loop state in the smallest stability region (in case the i = 1 model is correct so that the closed-loop state may not exit this region) and also indicate that the models will make noticeably different state predictions. To demonstrate this, we performed a discretization of the state and input spaces within a small range of the steady-state values, initialized each model from the discretized state values under the inputs in the input discretization, and simulated the three models for 0.01 h (checking that the Lyapunov function value did not exceed 300, which corresponds to ρ_1 ; the need to evaluate this over only 0.01 h of operation is because $\Delta = 0.01$ h will be used in the EMPC, and it is necessary that the state predictions from the different models are sufficiently different from one another after a sampling period that the models can be discriminated between at the end of a sampling period). The discretization used involved the following: initial conditions were developed by setting a variable $I_{discretize}$ that varied in increments of 0.1 between 0 and 0.5. Each initial condition for

 C_{Am} was then obtained by dividing the value of $I_{discretize}$ being used by 5, and each initial condition for T_m was then obtained by multiplying the value of $I_{discretize}$ being used by 20. The inputs were discretized so that C_{A0} varied from 2.5 to 5.5 kmol/m³ in increments of 0.1 kmol/m³ and Q varied from -10000 to 10000 kJ/h in increments of 1000 kJ/h. Examples of two sets of trajectories for C_{Am} and T_m are shown in Fig. 3, corresponding to two different sets of initial conditions and inputs selected within the discretization. Specifically, the top plots correspond to initial conditions of $C_{Am}=1.2231~\mathrm{kmol/m^3}$ and $T_m=438.25~\mathrm{K}$ with inputs of $C_{A0} = 3.9 \text{ kmol/m}^3$ and Q = 6000 kJ/h, whereas the bottom plots correspond to initial conditions of $C_{Am}=1.3231~\mathrm{kmol/m^3}$ and $T_m=448.25~\mathrm{K}$ with inputs of $C_{A0}=5.5~\mathrm{kmol/m^3}$ and Q=10000kJ/h. This figure shows that whereas it is difficult to discriminate between the models visually from the top plots, Model 1 is noticeably less accurate compared to the other two in the bottom plots. In particular, the absolute value of the difference between Model 1 and Model 2 at the end of the 0.1 h of operation in the top plots is $2.702 \times 10^{-5}~\mathrm{kmol/m^3}$ in C_{Am} and $0.0007~\mathrm{K}$ in T_m , whereas it is $0.001~\mathrm{kmol/m^3}$ in C_{Am} and 0.218 K in T_m in the bottom plots. The absolute value of the difference between Model 3 and Model 2 at the end of the 0.1 h of operation in the top plots is $3.657 \times 10^{-7} \text{ kmol/m}^3$ in C_{Am} and 0.0002 K in T_m , whereas it is 5.486×10^{-6} in C_{Am} and 0.0019 K in T_m in the bottom plots. This indicates that at least one of the models may eventually be able to be dropped from M_c under the control-assisted online model discrimination strategy, depending on the model error threshold set (if Model 1 is sufficiently accurate, it would be expected that the sensor measurements will be consistent with its trajectory and that the other two models could be dropped; if Models 2 or 3 are instead sufficiently accurate, it would be expected that the sensor measurements will be consistent with those trajectories and that Model 1 could be dropped). To see whether Models 2 and 3 and could be discriminated between if Model 1 was determined not to be sufficiently accurate and only those two models were left, further analysis would need to be performed. There is no guarantee that two models will be sufficiently different to be discriminated from one another online in the presence of measurement noise.

The EMPC is designed in a similar form to Eq. 11, in the sense that it uses the i=1 model at t_0 to establish constraints related to the Lyapunov function. Constraints in the spirit of Eqs. 11f-11g are formulated for this problem, where if $\hat{V}_1(x(t_k)) \leq \rho_{e,1}$, a constraint of the form in Eq. 11f is enforced at the end of each sampling period in the prediction horizon. If instead $\hat{V}_1(x(t_k)) > \rho_{e,1}$, a constraint of the

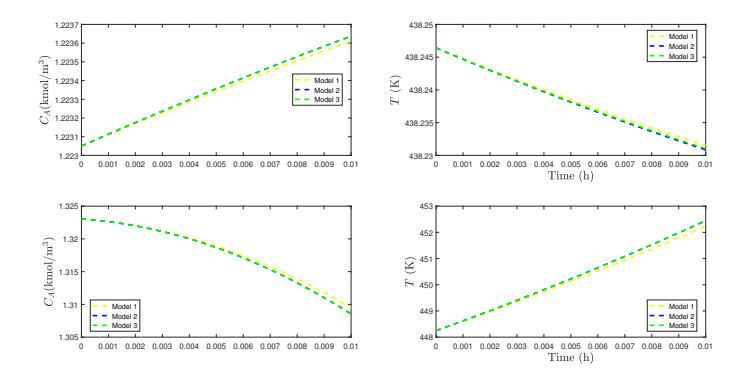


Figure 3: Maximum (plots from the bottom) and minimum (plots from the top) difference between the predicted state trajectories of the models over three sampling periods among a set of different initial conditions and inputs. The y-axis range is larger in the bottom plots than the top plots. Except in the upper right plot where the trajectory for Model 2 is somewhat visible on its own, the trajectories for Models 2 and 3 are overlaid.

form in Eq. 11g is used at t_k , and then a constraint of the form in Eqs. 11f is enforced at the end of each sampling period. Since the goal is to select a suitable mechanistic model in M_c , we explore the use of the form of the objective function of Eq. 11 with $\beta_1 = 0$, $\beta_2 = 1$, and $\gamma_{ij} = 1$, i = 1, 2 and j > i + 1 up to $|M_c|$, to attempt to maximize the distance between the state predictions from the three mechanistic model candidates in M_c (i.e., the LEMPC is implemented in data-gathering mode only). Particularly, the EMPC computes control actions (C_{A0} and Q) in a manner that seeks to maximize the following cost function:

$$\int_{t_k}^{t_{k+N}} 10^{-12} \sum_{i=1}^{2} \sum_{j=i+1}^{3} \left[(\tilde{x}_{q,1,i}(\tau) - \tilde{x}_{q,1,j}(\tau))^2 + (\tilde{x}_{q,2,i}(\tau) - \tilde{x}_{q,2,j}(\tau))^2 \right] d\tau \tag{33}$$

where $\tilde{x}_{q,1,i}$ and $\tilde{x}_{q,2,i}$ correspond to the predicted concentration of species A leaving the reactor and the outlet temperature of the reactor based on the i-th mechanistic model, respectively. The double sum in the objective function above was multiplied by 10^{-12} to avoid making the objective function magnitude too large.

To demonstrate aspects of EMPC-assisted model discrimination, the process state was initialized at the steady-state ($x_{init} = [0 \text{ kmol/m}^3 \text{ 0 K}]^T$) and the simulation was performed over 0.04 h of operation using a computer with an Lenovo model 80XN x64-based ideapad 320 with an Intel(R) Core(TM) i7-7500U CPU at 2.70 GHz, 2904 Mhz, running Windows 10 Enterprise, in MATLAB R2016b. N was set to 10. To simulate process disturbance and noise, the function "randn()" was used, with a seed to the random number generator, through the MATLAB function rng, of 10. To discriminate between the rival mechanistic models, we computed the following distance-based index $D_i = \sqrt{(\tilde{x}_{q,i}(t) - x(t))^2}$ (which reflects

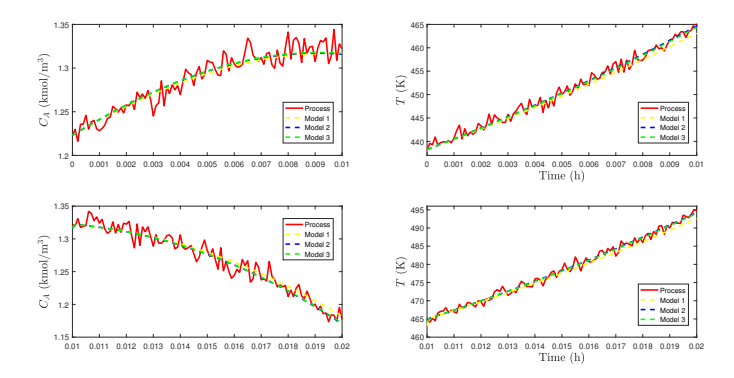


Figure 4: Measured closed-loop system trajectories ("Process") and predicted state trajectories ("Model 1," "Model 2," and "Model 3") using different mechanistic model candidates under the EMPC with the objective function in Eq. 33 from 0 to 0.01 h of operation (top plots) and from 0.01 to 0.02 h of operation (bottom plots). The predictions from Model 2 and Model 3 are almost overlaid.

the difference between the predicted closed-loop states, $\tilde{x}_{q,i}(t)$, based on the *i*-th model, i=1,2,3, and the measured states, x(t)) to evaluate the impact of setting different metrics for model discrimination and different thresholds ϵ_M on these metrics for discarding models during the model discrimination task. Fig. 4 shows the state predictions over the first and second 0.01 h of operation, reflecting differences between Model 1 and Models 2 and 3; however, due to the measurement noise and disturbances, the model which provides the best "fit" (or alternatively, which provides an insufficient "fit") to the process behavior is less clear visually. The controller drove the closed-loop state to operating data points off steady-state. The control actions computed by fmincon were not guaranteed to be global minima. In addition, over 0.04 h, the state predictions are kept inside their respective stability regions, which can be visualized in Fig. 6. For comparison, to evaluate whether any of the models might visually appear to be more accurate than others if the sensor noise is neglected, the predicted state trajectories from 0 to 0.01 h and 0.01 to 0.02 h are plotted against the process dynamic behavior in the absence of measurement noise (disturbances only) in Fig. 5. This figure indicates that Model 1 deviates more significantly from the process behavior than do the Model 2 and 3 predictions, indicating that understanding whether the EMPC-assisted technique could aid in distinguishing this in the presence of the measurement noise is desirable.

Because it is not clear visually which model, if any, provides a potential explanation for the process behavior in the presence of measurement noise, we return to the case with measurement noise and analyze the impact of different metrics on discriminating between the different models. The metrics to be analyzed are the norm of the difference between the state prediction from a model and the state measurement at the

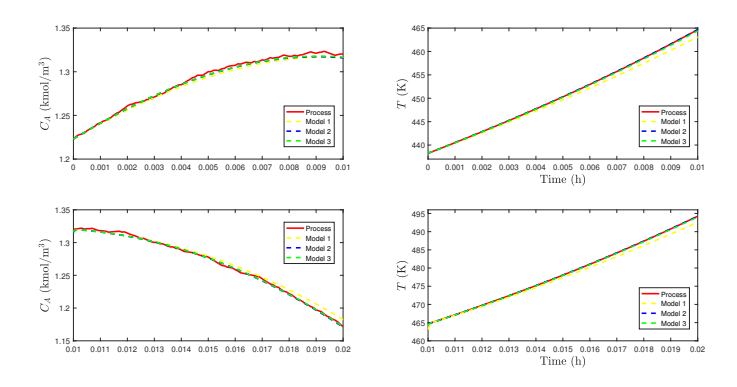


Figure 5: Measured closed-loop system trajectories in the absence of measurement noise ("Process") and predicted state trajectories ("Model 1," "Model 2," and "Model 3") using different mechanistic model candidates under the EMPC with the objective function in Eq. 33 from 0 to 0.01 h of operation (top plots) and from 0.01 to 0.02 h of operation (bottom plots). The predictions from Model 2 and Model 3 are almost overlaid.

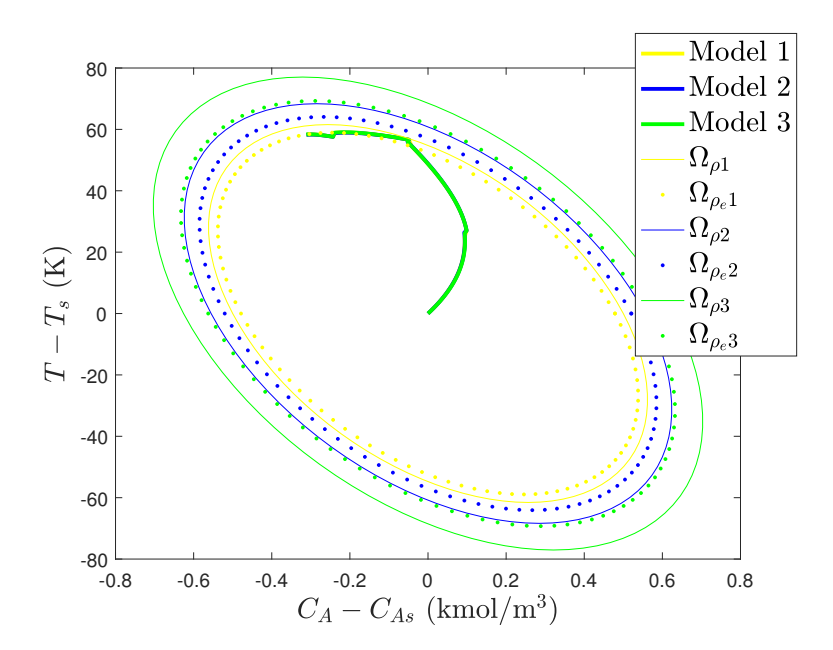


Figure 6: Trajectories of the state predictions for the three process models, initialized from a noisy measurement of the process state at the beginning of every sampling time, over 0.04 h for the three mechanistic model candidates under the EMPC with the objective function in Eq. 33.

end of a sampling period (Error Metric 1), the maximum value of the difference between the state prediction from a model and the state measurement at any point during a sampling period (Error Metric 2), and the average value of the difference between the state prediction from a model and the state measurement across a sampling period (Error Metric 3). Table 2 presents the results of using each metric in each of the four sampling periods simulated. It can be seen that in the first and second sampling periods, all three error metrics give a higher value for Model 1 compared to Models 2 and 3, though it is not as clear in the first sampling period with Error Metric 2. However, in later sampling periods, this is not always the case. For example, in sampling period 3 for Error Metric 2, Model 3 gives the largest value of the error metric. Except in the first sampling period for Error Metric 3, the value of the error metric for Model 2 is lower than the error metrics for the other models. However, the fact that this is not true in one sampling period indicates that error metrics and the thresholds on them must be carefully selected in practice to prevent discarding potentially reasonable models from M_c . These results also demonstrate that the measurement noise can make it challenging to discriminate between the models. Regarding the selection of thresholds, the data in Table 2 indicates that with different thresholds on the error, different models may have been kept or discarded from M_c . This discussion indicates that if the plant/model mismatch is large for all mechanistic models, various indexes for attempting to discriminate between models may all be large and potentially close to each other (from a theoretical perspective, it would have to be questioned whether any of them would then provide plant/model mismatch or bounded disturbances that are small enough to meet the stability requirements in Theorem 1).

To analyze the extent to which the difficulty in model discrimination in this example depends on the sensor noise, we can examine Error Metric 1 for the process with disturbances only (no measurement noise). In the first sampling period, it would evaluate to 1.537 for Model 1, 0.0105 for Model 2, and 0.251 for Model 3, and at the second sampling period it would be 1.659 for Model 1, 0.010 for Model 2, and 0.200 for Model 3, indicating that there is a large difference between Model 1 and Models 2 and 3 at these sampling periods. However, this difference is less noticeable in the third sampling period, where Error Metric 1 is 0.328 for Model 1, 0.180 for Model 2, and 0.345 for Model 3. This again indicates that working with model error and setting thresholds on model error when none of the process models postulated exactly replicates the dynamics, even in the absence of sensor noise, can be challenging in practice.

Table 2: Error metrics for different models for the four sampling periods from 0 to 0.04 h of operation using the EMPC with the objective function of Eq. 33 and the process with both measurement noise and disturbances considered.

Sampling	1	2	3	4
Period				
Error	Model 1: 1.854;	Model 1: 2.209;	Model 1: 1.372;	Model 1: 1.237;
Metric 1	Model 2: 0.308;	Model 2: 0.583;	Model 2: 1.177;	Model $2: 1.115;$
	Model $3: 0.568$	Model 3: 0.767	Model 3: 1.353	Model 3: 1.232
Error	Model 1: 2.795;	Model 1: 3.096;	Model 1: 2.621;	Model 1: 2.563;
Metric 2	Model 2: 2.467;	Model 2: 2.322;	Model 2: 2.482;	Model 2: 2.536 ;
	Model 3: 2.495	Model 3: 2.413	Model 3: 2.632	Model 3: 2.580
Error	Model 1: 0.986;	Model 1: 1.025;	Model 1: 0.929;	Model 1: 0.684;
Metric 3	Model 2: 0.785;	Model 2: 0.784;	Model 2: 0.921;	Model $2: 0.680;$
	Model 3: 0.783	Model 3: 0.789	Model 3: 0.939	Model 3: 0.684

The example above used the EMPC only in data-gathering mode; to attempt to avoid profit loss during the model discrimination task, we can evaluate whether an economics-based objective function can be used instead. To evaluate this case, an EMPC using an economics-based objective function (to be referred to subsequently as "standard EMPC" because it uses an economics-based objective function which is a standard goal of EMPC when model discrimination is not in view) may be implemented to attempt to obtain the desired mechanistic model discrimination. Conceptually, if a standard LEMPC operates the process in a manner that causes a dynamic/transient system behavior, profit-maximizing operation may already impose enough "excitation" to the system so that new information can be gathered for model discrimination. In this case, the objective function based solely on data collection ($\beta_2 = 1$) may not be needed to select a suitable mechanistic model in M_c , which could lead to profit loss compared to the case where an economics-based objective function is used throughout the time of operation.

To investigate this with the set of models M_c defined above, we carried out the process simulation under the standard LEMPC over 0.04 h of operation with $x_{init} = [0 \text{ kmol/m}^3 \text{ 0 K}]^T$. For this control formulation, Δ and N were again set to 0.01 h and 10, respectively, and the Lyapunov-based stability constraints were designed using the same method as described above for when the objective function was given by Eq. 33. The standard LEMPC's economics-based objective function was formulated to maximize sum of the production rates from each model as follows:

$$\int_{t_k}^{t_{k+N}} \left[\sum_{i=1}^{3} k_0 e^{-E/(R(\tilde{x}_{q,2,i} + T_{ms}))} (\tilde{x}_{q,1,i} + C_{Ams})^2 \right] d\tau$$
 (34)

Over the first 0.04 h of operation, Error Metric 1 evaluated to the same values at the end of the sampling periods as it did in Table 2 for the case that the EMPC with the objective function in Eq. 33 was used. In general, this can happen, because the inputs which maximize one objective function may also maximize another. This motivates attempting to start model discrimination with $\beta_1 = 1$ and $\beta_2 = 0$, and then using $\beta_2 = 1$ if the data when $\beta_2 = 0$ is insufficient for model discrimination.

5. Conclusion

This work highlights a capability of LEMPC to operate a process in a flexible and potentially non-routine fashion to meet online operating goals, in particular for discriminating between mechanistic model candidates. The LEMPC developed for this task determines what desired data should be gathered for model discrimination and can collect the required information while maintaining closed-loop stability even when it is unknown which of a set of model candidates may be sufficiently accurate. A chemical process example was used to demonstrate practical considerations for EMPC-assisted online model discrimination.

6. Acknowledgements

Financial support from the National Science Foundation CBET-1839675, the Air Force Office of Scientific Research under award number FA9550-19-1-0059, and Wayne State University is gratefully acknowledged.

Literature Cited

- [1] M. Ellis, H. Durand, P. D. Christofides, A tutorial review of economic model predictive control methods, Journal of Process Control 24 (2014) 1156–1178.
- [2] E. A. del Rio-Chanona, D. Zhang, V. S. Vassiliadis, Model-based real-time optimisation of a fed-batch cyanobacterial hydrogen production process using economic model predictive control strategy, Chemical engineering science 142 (2016) 289–298.
- [3] A. Gopalakrishnan, L. T. Biegler, Economic nonlinear model predictive control for periodic optimal operation of gas pipeline networks, Computers & Chemical Engineering 52 (2013) 90–99.

- [4] R. Halvgaard, N. K. Poulsen, H. Madsen, J. B. Jørgensen, Economic model predictive control for building climate control in a smart grid, in: 2012 IEEE PES innovative smart grid technologies (ISGT), IEEE, 2012, pp. 1–6.
- [5] L. Giuliani, H. Durand, Data-based nonlinear model identification in economic model predictive control, Smart and Sustainable Manufacturing Systems 2 (2018) 20180025.
- [6] T. Gamer, M. Hoernicke, B. Kloepper, R. Bauer, A. J. Isaksson, The autonomous industrial plant-future of process engineering, operations and maintenance, IFAC-PapersOnLine 52 (1) (2019) 454–460.
- [7] M. Von Stosch, R. Oliveira, J. Peres, S. F. de Azevedo, Hybrid semi-parametric modeling in process systems engineering: Past, present and future, Computers & Chemical Engineering 60 (2014) 86–101.
- [8] O. Kahrs, W. Marquardt, The validity domain of hybrid models and its application in process optimization, Chemical Engineering and Processing: Process Intensification 46 (11) (2007) 1054–1066.
- [9] N. Bhutani, G. Rangaiah, A. Ray, First-principles, data-based, and hybrid modeling and optimization of an industrial hydrocracking unit, Industrial & engineering chemistry research 45 (23) (2006) 7807– 7816.
- [10] S. Olofsson, E. S. Schultz, A. Mhamdi, A. Mitsos, M. P. Deisenroth, R. Misener, Design of dynamic experiments for black-box model discrimination, arXiv preprint arXiv:2102.03782 (2021).
- [11] P. Schrangl, P. Tkachenko, L. Del Re, Iterative model identification of nonlinear systems of unknown structure: Systematic data-based modeling utilizing design of experiments, IEEE Control Systems Magazine 40 (3) (2020) 26–48.
- [12] C. Waldron, A. Pankajakshan, M. Quaglio, E. Cao, F. Galvanin, A. Gavriilidis, Closed-loop model-based design of experiments for kinetic model discrimination and parameter estimation: Benzoic acid esterification on a heterogeneous catalyst, Industrial & Engineering Chemistry Research 58 (49) (2019) 22165–22177.
- [13] A. C. Atkinson, V. V. Fedorov, Optimal design: Experiments for discriminating between several models, Biometrika 62 (2) (1975) 289–303.

- [14] T. Tajsoleiman, Automating experimentation in miniaturized reactors, Ph.D. thesis (2018).
- [15] B. Melykuti, E. August, A. Papachristodoulou, H. El-Samad, Discriminating between rival biochemical network models: three approaches to optimal experiment design, BMC systems biology 4 (1) (2010) 1–16.
- [16] T. A. N. Heirung, B. Erik Ydstie, B. Foss, Towards dual mpc, IFAC Proceedings Volumes 45 (17) (2012) 502–507.
- [17] K. Kumar, S. C. Patwardhan, S. Noronha, An adaptive dual mpc scheme based on output error models parameterized using generalized orthonormal basis filters, IFAC-PapersOnLine 50 (1) (2017) 9077–9082.
- [18] H. Genceli, M. Nikolaou, New approach to constrained predictive control with simultaneous model identification, AIChE journal 42 (10) (1996) 2857–2868.
- [19] T. A. N. Heirung, A. Mesbah, Stochastic nonlinear model predictive control with active model discrimination: a closed-loop fault diagnosis application, IFAC-PapersOnLine 50 (1) (2017) 15934–15939.
- [20] T. Lew, A. Sharma, J. Harrison, A. Bylard, M. Pavone, Safe active dynamics learning and control: A sequential exploration-exploitation framework, arXiv preprint arXiv:2008.11700 (2020).
- [21] R. Cheng, G. Orosz, R. M. Murray, J. W. Burdick, End-to-end safe reinforcement learning through barrier functions for safety-critical continuous control tasks, in: Proceedings of the AAAI Conference on Artificial Intelligence, Vol. 33, 2019, pp. 3387–3395.
- [22] T. Koller, F. Berkenkamp, M. Turchetta, A. Krause, Learning-based model predictive control for safe exploration, in: 2018 IEEE Conference on Decision and Control (CDC), IEEE, 2018, pp. 6059–6066.
- [23] M. Heidarinejad, J. Liu, P. D. Christofides, Economic model predictive control of nonlinear process systems using Lyapunov techniques, AIChE Journal 58 (2012) 855–870.
- [24] M. Ellis, H. Durand, P. D. Christofides, A tutorial review of economic model predictive control methods, Journal of Process Control 24 (2014) 1156–1178.

- [25] M. Kheradmandi, P. Mhaskar, Adaptive model predictive batch process monitoring and control, Industrial & Engineering Chemistry Research 57 (43) (2018) 14628–14636.
- [26] J. B. Rawlings, D. Angeli, C. N. Bates, Fundamentals of economic model predictive control, in: 2012
 IEEE 51st IEEE conference on decision and control (CDC), IEEE, 2012, pp. 3851–3861.
- [27] L. Fagiano, A. R. Teel, Generalized terminal state constraint for model predictive control, Automatica 49 (9) (2013) 2622–2631.
- [28] M. A. Müller, L. Grüne, Economic model predictive control without terminal constraints for optimal periodic behavior, Automatica 70 (2016) 128–139.
- [29] F. A. Bayer, M. A. Müller, F. Allgöwer, On optimal system operation in robust economic mpc, Automatica 88 (2018) 98–106.
- [30] L. Schwenkel, J. Köhler, M. A. Müller, F. Allgöwer, Robust economic model predictive control without terminal conditions, IFAC-PapersOnLine 53 (2) (2020) 7097–7104.
- [31] M. Ellis, J. Zhang, J. Liu, P. D. Christofides, Robust moving horizon estimation based output feedback economic model predictive control, Systems & Control Letters 68 (2014) 101–109.
- [32] T. Homer, M. Mahmood, P. Mhaskar, A trajectory-based method for constructing null controllable regions, International Journal of Robust and Nonlinear Control 30 (2) (2020) 776–786.
- [33] T. Homer, P. Mhaskar, Utilizing null controllable regions to stabilize input-constrained nonlinear systems, Computers & Chemical Engineering 108 (2018) 24–30.
- [34] M. Mahmood, T. Homer, P. Mhaskar, Controllability minimum principle based construction of the null controllable region for nonlinear systems, International Journal of Robust and Nonlinear Control (2021).